INTERNATIONAL JOURNAL FOR NUMERICAL METHODS IN FLUIDS, VOL. 18, 1153–1165 (1994)

ON THE IMPLEMENTATION OF SYMMETRIC AND ANTISYMMETRIC PERIODIC BOUNDARY CONDITIONS FOR INCOMPRESSIBLE FLOW

GUUS SEGAL, KEES VUIK AND KEES KASSELS

Delft University of Technology, Faculty of Technical Mathematics and Informatics, P.O. Box 5031, 2500 GA Delft, The Netherlands

SUMMARY

In this paper we consider symmetric and antisymmetric periodic boundary conditions for flows governed by the incompressible Navier–Stokes equations. Classical periodic boundary conditions are studied as well as symmetric and antisymmetric periodic boundary conditions in which there is a pressure difference between inlet and outlet. The implementation of this type of boundary conditions in a finite element code using the penalty function formulation is treated and also the implementation in a finite volume code based on pressure correction. The methods are demonstrated by computation of a flow through a staggered tube bundle.

KEY WORDS Navier–Stokes Incompressible flow Finite element method Finite volume method Periodic boundary condition

1. INTRODUCTION

In many papers and text books[1–8] discretizations of the incompressible Navier–Stokes equations are described, but in general not much attention is paid to the incorporation of boundary conditions. However, for engineering applications the implementation of adequate boundary conditions is equally important for accuracy as the formulation and discretization of the differential equations itself. In this paper we shall consider three types of periodic and antiperiodic boundary conditions, namely

(i) periodicity in velocity and pressure
(ii) periodicity in velocity and pressure gradient
(iii) antisymmetric periodicity in velocity and pressure gradient.

The last two boundary conditions are combined with prescription of a given flow rate.

Pure periodic boundary conditions arise for example in the case of an artificial cut in a region. Such artificial cuts naturally arise in the computation of a flow around an obstacle by finite volume techniques.

Periodicity in velocity and pressure gradient in combination with a prescribed flow rate naturally arises in the case of a periodically repeated configuration.

For example, experiments in a bundle of seven horizontal staggered pipes (Figure 1) by Simonin and Barcouda[7] show that for water flowing upwards at an average velocity of 1·06 m s^{-1} the flow becomes periodic around the fourth row from the bottom. Hence for the flow in the interior it suffices to compute the flow in the dashed computational region only. In this example

CCC 0271–2091/94/121153–13

Received July 1993
Revised December 1993

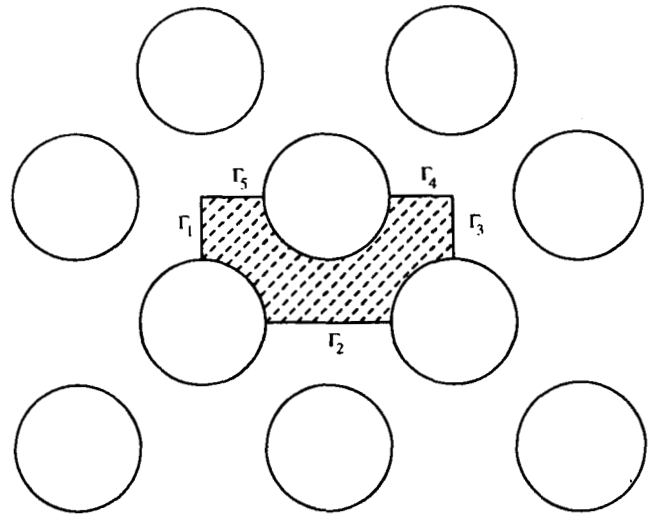

Figure 1. Computational region in array of staggered pipes with periodic boundary conditions

the boundaries Γ_2, Γ_4 and Γ_5 are symmetry boundaries, whereas Γ_1 and Γ_3 are periodic boundaries. In order to have a flow, it is necessary that the pressures at the left-hand side and right-hand sides differ by a constant. This unknown constant may be given implicitly by prescribing the flow rate Q.

In this particular problem it is possible to reduce the computational domain still further by halving, as shown in Figure 2. In this case the boundary conditions at the boundaries Γ_1 and Γ_3 are antisymmetric periodic instead of symmetric.

Periodic boundary conditions with a given flow rate in combination with finite element methods have been treated by Fortin.[2] He uses an Uzawa-type scheme to solve the incompress-

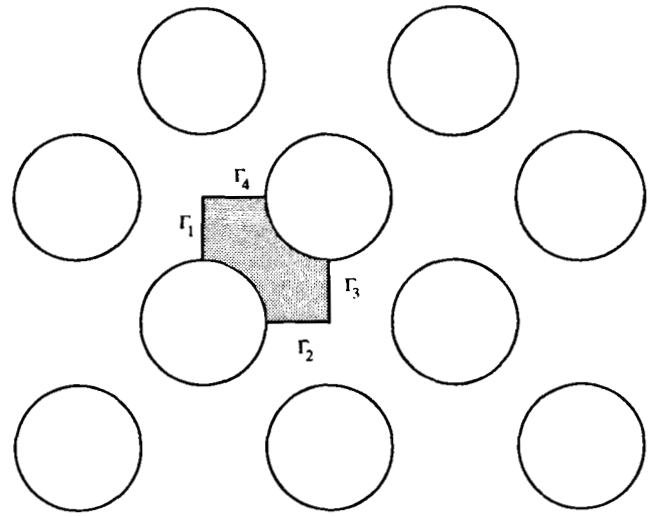

Figure 2. Computational region in array of staggered pipes with antiperiodic boundary conditions

ible Navier–Stokes equations. We shall extend his ideas to antiperiodic boundary conditions in combination with a penalty function formulation.

Perić[5] treats antisymmetric periodic boundary conditions in combination with a finite volume method. He uses artificial cells at the inlet and outlet which are copies of the cells at the other side. Starting with some initial field, the flow at the next time step is computed. As boundary conditions at inlet and outlet the computed velocities at the corresponding other sides are copied from the preceding iteration. By iterating, this process converges to the correct values. However, this process requires approximately two to three times the usual number of iterations.

2. FORMULATION OF THE PROBLEM

We consider the non-stationary incompressible Navier–Stokes equations in general co-ordinates,

$$\frac{\partial}{\partial t}(\rho U^{\alpha}) + (\rho U^{\alpha} U^{\beta})_{,\beta} + (g^{\alpha\beta} p)_{,\beta} - \tau^{\alpha\beta}_{,\beta} = \rho f^{\alpha}, \tag{1}$$

$$U^{\alpha}_{,\alpha} = 0, \tag{2}$$

where $\tau^{\alpha\beta}$ represents the deviatoric stress tensor

$$\tau^{\alpha\beta} = \mu(g^{\alpha\gamma} U^{\beta}_{,\gamma} + g^{\gamma\beta} U^{\alpha}_{,\gamma}), \tag{3}$$

with μ the viscosity, p the pressure, U^{α} the contravariant velocity component and ρ the density of the fluid. In the formulation the standard tensor notation with summation convention is used; $g^{\alpha\beta}$ represents the metric tensor. See References 3, 4, 6 and 9 for details. In our present study we restrict ourselves to laminar, stationary flow although the work is motivated by a turbulent problem.

For the sake of argument we restrict ourselves to a rectangular domain as shown in Figure 3 with periodicity at the inlet and outlet boundaries Γ_1 and Γ_3. We consider the following types of periodicity.

Pure periodicity

In this case the boundary conditions are given by

$$\mathbf{u}_{\text{left}} = \mathbf{u}_{\text{right}}, \qquad p_{\text{left}} = p_{\text{right}},$$
$$\frac{\partial \mathbf{u}}{\partial n}\Big|_{\text{left}} = -\frac{\partial \mathbf{u}}{\partial n}\Big|_{\text{right}}, \tag{4}$$

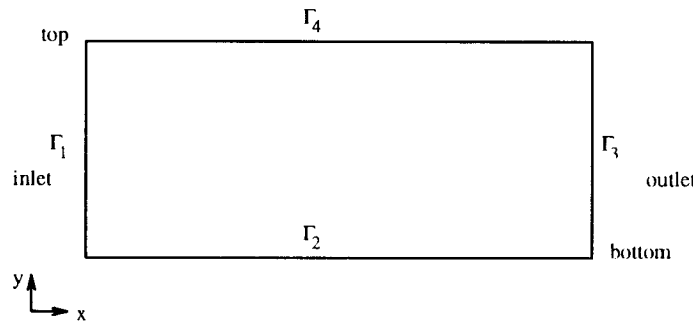

Figure 3. Periodicity at a rectangular domain

where $\mathbf{u}$ is the velocity vector and n is the outward-directed normal. The subscripts 'left' and 'right' indicate that the values at the left- and right-hand sides respectively are meant. Of course $\mathbf{u}$ and p may vary along these boundaries.

Periodicity with unknown jump in pressure

The boundary conditions for the velocity are the same as in (4), but there is a constant pressure difference between the left- and right-hand sides. Thus

$$\mathbf{u}_{\text{left}} = \mathbf{u}_{\text{right}}, \tag{5a}$$

$$\frac{\partial \mathbf{u}}{\partial n}\Big|_{\text{left}} = -\frac{\partial \mathbf{u}}{\partial n}\Big|_{\text{right}}, \tag{5b}$$

$$p_{\text{left}} = p_{\text{right}} + c. \tag{5c}$$

To fix the unknown constant c, an extra condition is necessary. It is quite natural to prescribe the flow rate Q as

$$Q = -\int_{\Gamma_l} \mathbf{u}\cdot\mathbf{n}\, d\Gamma. \tag{6}$$

Antisymmetric periodicity with unknown jump in pressure

This boundary condition very much resembles that of (5a)–(5c) and (6). However, the tangential velocity component and the tangential direction get opposite signs. Hence

$$\mathbf{u}\cdot\mathbf{n}(y)|_{\text{left}} = \mathbf{u}\cdot\mathbf{n}(y_{\text{top}} - y)|_{\text{right}}, \tag{7a}$$

$$\mathbf{u}\cdot\mathbf{t}(y)|_{\text{left}} = -\mathbf{u}\cdot\mathbf{t}(y_{\text{top}} - y)|_{\text{right}}, \tag{7b}$$

$$\frac{\partial \mathbf{u}\cdot\mathbf{n}}{\partial n}(y)|_{\text{left}} = -\frac{\partial \mathbf{u}\cdot\mathbf{n}}{\partial n}(y_{\text{top}} - y)|_{\text{right}}, \tag{7c}$$

$$\frac{\partial \mathbf{u}\cdot\mathbf{t}}{\partial n}(y)|_{\text{left}} = \frac{\partial \mathbf{u}\cdot\mathbf{t}}{\partial n}(y_{\text{top}} - y)|_{\text{right}}, \tag{7d}$$

$$p(y)|_{\text{left}} = p(y_{\text{top}} - y)|_{\text{right}} + c, \tag{7e}$$

where $\mathbf{t}$ is the tangential vector, which is taken from bottom to top. Furthermore, condition (6) holds.

3. SOLUTION BY FINITE ELEMENT TECHNIQUES

To solve the incompressible Navier–Stokes equations, the standard Galerkin approach (SGA) is applied in this section. We restrict ourselves to extended quadratic triangles of Crouzeix–Raviart type.[1] Hence the velocity per element is approximated by an extended quadratic polynomial and the pressure per element is a linear discontinuous polynomial.

Table II. The three PVM configurations used in the experiments

	Workstation	Relative speed
PVM configuration A		
Host	DECstation 5000	2
Frontal	DECstation 5000	2
Node 1: element contributions	DECstation 3100 A	1
Node 2: element contributions	DECstation 3100 B	1
Node 3: element contributions	DECstation 3100 C	1
PVM configuration B		
Host	DECstation 5000	2
Frontal	DECstation 5000	2
Node 1: element contributions	DECstation 5000	2
Node 2: element contributions	DECstation 3100 A	1
Node 3: element contributions	DECstation 3100 B	1
Node 4: element contributions	DECstation 3100 C	1
PVM configuration C		
Host	SG IRIS	5
Frontal	SG IRIS	5
Node 1: element contributions	SG IRIS	5
Node 2: element contributions	DECstation 5000	4
Node 3: element contributions	DECstation 3100 A	2
Node 4: element contributions	DECstation 3100 B	2
Node 5: element contributions	DECstation 3100 C	2
Node 6: element contributions	DG 200 A	1
Node 7: element contributions	DG 200 B	1

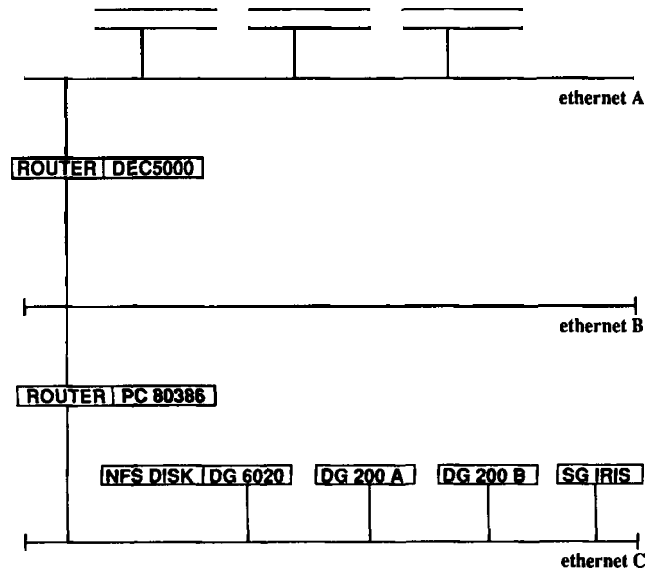

Figure 6. Network topology of workstations used in this work

In the case of a stationary Stokes equation the discretization of equations (1)–(3) under the constraint (12) may be regarded as a minimization problem of the form

$$\min_{\mathbf{u}} \tfrac{1}{2}\mathbf{u}^{\mathrm{T}}\mathbf{S}\mathbf{u} - \mathbf{u}^{\mathrm{T}}\mathbf{F} \tag{13a}$$

under the constraints

$$\mathbf{L}\mathbf{u} = \mathbf{0}, \tag{13b}$$

$$\mathbf{R}\mathbf{u} = Q. \tag{13c}$$

Here **Su** represents the discretization of the stress tensor, **F** the discretization of the right-hand side and **Lu** = **0** the discretization of the continuity equation.

One immediately shows that the Kuhn–Tucker relations associated with (13a)–(13c) can be formulated as

$$\mathbf{S}\mathbf{u} + \mathbf{L}^{\mathrm{T}}\mathbf{p} + \mathbf{R}^{\mathrm{T}}\lambda = \mathbf{F}, \tag{14a}$$

$$\mathbf{L}\mathbf{u} = \mathbf{0}, \tag{14b}$$

$$\mathbf{R}\mathbf{u} = Q. \tag{14c}$$

In the case of a continuous pressure approximation with pressure unknowns at the boundary of the element (Taylor–Hood element) the parameter λ may easily be identified with the unknown constant c in (7e). In the case of a discontinuous pressure approximation such an identification is no longer clear, although one may expect a strong relation between λ and c.

From (13a)–(13c) it is quite trivial that the penalty function formulation of the stationary Navier–Stokes equations under the constraint (12) becomes

$$\mathbf{S}\mathbf{u} + \mathbf{N}(\mathbf{u})\mathbf{u} + \sigma_1\mathbf{L}^{\mathrm{T}}\mathbf{L}\mathbf{u} + \sigma_2\mathbf{R}^{\mathrm{T}}\mathbf{R}\mathbf{u} = \mathbf{F} + \sigma_2\mathbf{R}^{\mathrm{T}}Q, \tag{15}$$

where σ_1 and σ_2 are penalty parameters and **N(u)u** denotes the discretization of the convection terms.

The matrix $\sigma_2\mathbf{R}^{\mathrm{T}}\mathbf{R}$ and the right-hand side term $\sigma_2\mathbf{R}^{\mathrm{T}}Q$ are built using an element containing all normal components of the velocity at the inlet. The boundary conditions for the pressure are satisfied implicitly by formulation (15).

4. SOLUTION BY FINITE VOLUME TECHNIQUES

Our finite volume discretization of the incompressible Navier–Stokes equations is based on a boundary-fitted staggered approach as described in References 3, 4, 6 and 10. The curved grid is mapped on to a rectangular domain and the invariant formulation (1)–(3) of the Navier–Stokes equations is used. With respect to the mapping it is supposed that only co-ordinates of the vertices of the cells are known. All geometrical coefficients including Christoffel symbols are computed by finite differences of the co-ordinates. In order to decouple velocity and pressure computation, a standard pressure correction method as described by Van Kan[10] is used. The non-linear equations are linearized by a standard Newton linearization and the systems of linear equations are solved by a preconditioned GMRESR method.[11]

The position of the unknowns in the staggered grid in the computational domain is sketched in Figure 4.

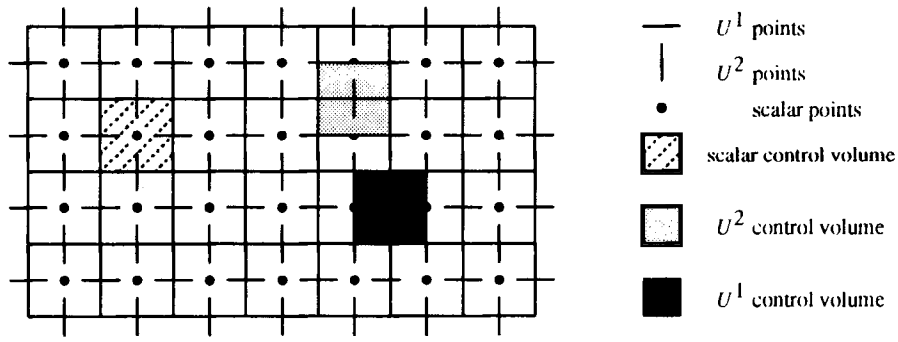

Figure 4. Position of unknowns in staggered grid

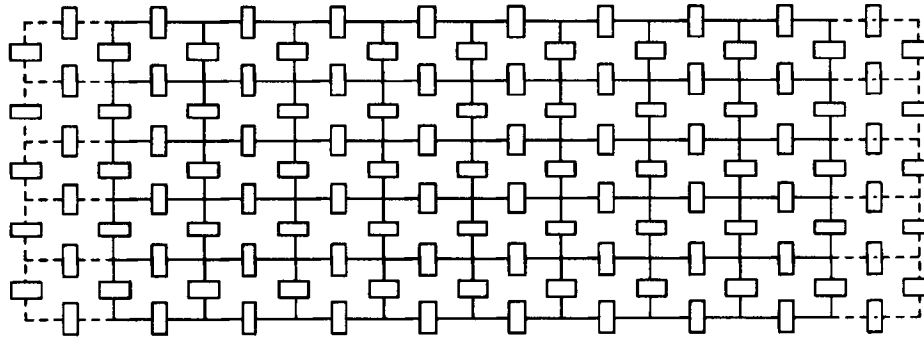

Figure 5. Extension of computational domain with virtual cells

In order to incorporate the periodic boundary condition (5a) or the antisymmetric boundary condition (7a), the equations for the normal velocity components at the inlet boundary are replaced by trivial equations making the velocity components of the left- and right-hand sides identical:

$$\mathbf{u}\cdot\mathbf{n}|_{\text{inlet}} = \mathbf{u}\cdot\mathbf{n}|_{\text{outlet}}. \tag{16}$$

In the antisymmetric case of course the correct unknowns must be coupled. In order to prescribe the other types of periodic boundary conditions, at both the left- and right-hand sides a column of virtual cells is introduced (see Figure 5).

The virtual unknowns in the virtual cells, however, are in fact the real unknowns at the other side taking the possible antisymmetry into account. Of course in the virtual pressure unknowns it is necessary to incorporate the unknown pressure jump constant c from equation (5c). The standard finite volume method is applied for all internal velocity unknowns, but also for the normal components at the outlet boundary.

In this way we get the following system of non-stationary non-linear equations:

$$\mathbf{Mu} + \mathbf{Su} + \mathbf{N(u)u} + \mathbf{G}^{\mathrm{T}}\mathbf{p} + \bar{\mathbf{G}}^{\mathrm{T}}c = \mathbf{F}, \tag{17a}$$

$$\mathbf{Du} = 0, \tag{17b}$$

$$\mathbf{Ru} = Q. \tag{17c}$$

$\mathbf{Su}$, $\mathbf{N(u)u}$, $\mathbf{Ru} = Q$ and $\mathbf{F}$ have exactly the same meaning as in (14a)–(14c), although their contents are completely different. $\mathbf{G}^T\mathbf{p}$ represents the discretization of ∇p except for the unknown constant, whose contribution is stored in $\bar{\mathbf{G}}^T c$. Note that the matrix $\bar{\mathbf{G}}$ has only non-zero entries in the points connected to inflow and outflow boundaries. $\mathbf{Du} = \mathbf{0}$ gives the discretization of the continuity equation and $\mathbf{Mu}$ the discretization of the time derivative. In fact $\mathbf{M}$ is a diagonal matrix containing the value of ρ multiplied by the area of the corresponding control volume as diagonal elements.

In order to solve equations (17a)–(17c), the standard Newton linearization is applied. Furthermore, we extend the pressure correction method as described by Van Kan[10] in order to incorporate the unknown c and the extra equation (17c).

If we apply a standard θ-method to (17a)–(17c), we get the following system of non-linear equations:

$$\mathbf{M}\frac{\mathbf{u}^{n+1}-\mathbf{u}^n}{\Delta t} + \theta\tilde{\mathbf{S}}\mathbf{u}^{n+1} + (1-\theta)\tilde{\mathbf{S}}\mathbf{u}^n + \theta\mathbf{G}^T\mathbf{p}^{n+1} + (1-\theta)\mathbf{G}^T\mathbf{p}^n + \theta\bar{\mathbf{G}}^T c^{n+1} + (1-\theta)\bar{\mathbf{G}}^T c^n = \theta\tilde{\mathbf{F}}^{n+1} + (1-\theta)\tilde{\mathbf{F}}^n, \tag{18a}$$

$$\mathbf{Du}^{n+1} = \mathbf{0}, \tag{18b}$$

$$\mathbf{Ru}^{n+1} = 0. \tag{18c}$$

Here $\tilde{\mathbf{S}}$ denotes the contribution of $\mathbf{S}$ and the matrix part of the linearization of $\mathbf{N(u)u}$. The right-hand-side part of the linearization is put into the term $\tilde{\mathbf{F}}$.

Now we follow the usual approach with respect to pressure correction, where we treat the constant c in exactly the same way as the pressure $\mathbf{p}$. Hence in equation (18a) $\mathbf{u}^{n+1}$ is replaced by a predictor $\mathbf{u}^*$ and $\mathbf{p}$ and c are only introduced at the preceding time level:

$$\mathbf{M}\frac{\mathbf{u}^*-\mathbf{u}^n}{\Delta t} + \theta\tilde{\mathbf{S}}\mathbf{u}^* + (1-\theta)\tilde{\mathbf{S}}\mathbf{u}^n + \mathbf{G}^T\mathbf{p}^n + \bar{\mathbf{G}}^T c^n = \tilde{\mathbf{F}}^{n+\theta}, \tag{19}$$

in which $\tilde{\mathbf{F}}^{n+\theta} = \theta\tilde{\mathbf{F}}^{n+1} + (1-\theta)\tilde{\mathbf{F}}^n$. The velocity field $\mathbf{u}^*$ does not only have to be projected on the space of divergence-free vector fields but also on those fields satisfying (17c). For this reason (19) is subtracted from (18a) and all terms involving $\tilde{\mathbf{S}}$ are neglected just as in the standard pressure correction method. This yields

$$\mathbf{M}\frac{\mathbf{u}^{n+1}-\mathbf{u}^*}{\Delta t} + \theta\mathbf{G}^T(\mathbf{p}^{n+1}-\mathbf{p}^n) + \theta\bar{\mathbf{G}}^T(c^{n+1}-c^n) = \mathbf{0}. \tag{20}$$

If we premultiply equation (20) by $\mathbf{DM}^{-1}$ and $\mathbf{RM}^{-1}$ respectively and apply equations (18b) and (18c), we get

$$-\frac{\mathbf{Du}^*}{\Delta t} + \theta\mathbf{DM}^{-1}\mathbf{G}^T(\mathbf{p}^{n+1}-\mathbf{p}^n) + \theta\mathbf{DM}^{-1}\bar{\mathbf{G}}^T(c^{n+1}-c^n) = 0, \tag{21}$$

$$\frac{Q-\mathbf{Ru}^*}{\Delta t} + \theta\mathbf{RM}^{-1}\mathbf{G}^T(\mathbf{p}^{n+1}-\mathbf{p}^n) + \theta\mathbf{RM}^{-1}\bar{\mathbf{G}}^T(c^{n+1}-c^n) = 0. \tag{22}$$

Since $\theta \mathbf{R}\mathbf{M}^{-1}\bar{\mathbf{G}}^{\mathrm{T}}$ is a number, $c^{n+1} - c^n$ may be eliminated from (22) in order to get

$$c^{n+1} - c^n = \frac{-1}{\theta \mathbf{R}\mathbf{M}^{-1}\bar{\mathbf{G}}^{\mathrm{T}}} \left(\theta \mathbf{R}\mathbf{M}^{-1}\mathbf{G}^{\mathrm{T}}(\mathbf{p}^{n+1} - \mathbf{p}^n) + \frac{Q - \mathbf{R}\mathbf{u}^*}{\Delta t} \right), \tag{23a}$$

$$\theta \mathbf{D}\mathbf{M}^{-1} \left(\mathbf{G}^{\mathrm{T}} - \frac{\bar{\mathbf{G}}^{\mathrm{T}}\mathbf{R}\mathbf{M}^{-1}\mathbf{G}^{\mathrm{T}}}{\mathbf{R}\mathbf{M}^{-1}\bar{\mathbf{G}}^{\mathrm{T}}} \right) (\mathbf{p}^{n+1} - \mathbf{p}^n) = \frac{\mathbf{D}\mathbf{u}^*}{\Delta t} + \frac{\mathbf{D}\mathbf{M}^{-1}\bar{\mathbf{G}}^{\mathrm{T}}}{\mathbf{R}\mathbf{M}^{-1}\bar{\mathbf{G}}^{\mathrm{T}}} \frac{Q - \mathbf{R}\mathbf{u}^*}{\Delta t}. \tag{23b}$$

Equation (23b) is a modified Laplacian-type equation to compute the pressure correction. From this correction $c^{n+1} - c^n$ is computed by (23a) and finally $\mathbf{u}^{n+1} - \mathbf{u}^n$ from (20).

Since we use an iterative linear solver, it is not necessary to compute the matrix $\mathbf{D}\mathbf{M}^{-1}(\bar{\mathbf{G}}^{\mathrm{T}} - \bar{\mathbf{G}}^{\mathrm{T}}\mathbf{R}\mathbf{M}^{-1}\mathbf{G}^{\mathrm{T}}/\mathbf{R}\mathbf{M}^{-1}\bar{\mathbf{G}}^{\mathrm{T}})$ explicitly. It is sufficient to programme the corresponding matrix–vector multiplication. This is an important observation, since the computed matrix is a full matrix whereas each of its submatrices is very sparse. With respect to the preconditioning we limit ourselves to an incomplete LU decomposition of the matrix $\mathbf{D}\mathbf{M}^{-1}$. The numerical experiments treated in Section 5 indicate that it is a rather good preconditioner.

5. A NUMERICAL EXAMPLE

In order to test the methods described in Sections 3 and 4, we consider a flow of water across a bundle of staggered pipes as shown in Figure 1. The computational region as plotted in Figure 2 is considered, which means that the antisymmetric periodic conditions must be applied.

The diameter of the pipes is 10·85 mm and the distance between the centroids of neighbouring pipes is 45 mm in both the horizontal and vertical directions. The mean velocity V_0 (from left to right) at the inlet is 1·06 m s^{-1}, which implies that the flow rate is given by $Q = 0{\cdot}01235$ m^3 s^{-1}. The Reynolds number Re_D is related to the diameter D of the pipes. Following Perić,[5] who solved a similar problem, the flow has been computed for three Reynolds numbers, $Re_D = 15$, 45 and 140.

Figure 6 shows the finite element mesh used, including the connection elements, which were introduced because of the antisymmetric periodicity. The corresponding finite volume grid is shown in Figure 7.

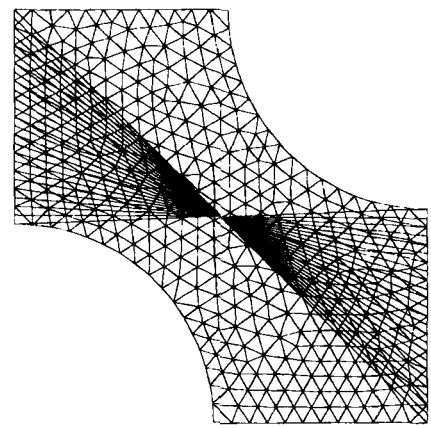

Figure 6. Finite element mesh for staggered tube problem, including connection elements

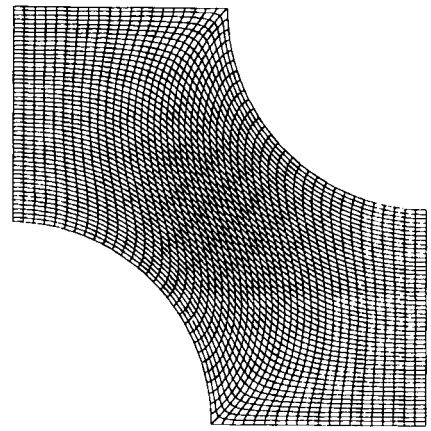

Figure 7. Finite volume grid for staggered tube problem

The finite element method has been solved using a penalty method and a direct linear solver (profile method). In this stationary code four ($Re_D = 15$) to six ($Re_D = 140$) Newton iterations were necessary to converge to the final solution.

Figure 8 shows the computed streamlines for $Re_D = 140$ and Figure 9 the corresponding isobars. In order to get a clearer view of the flow and pressure distribution, the computed results have been copied to a region consisting of four computational blocks.

Of course in the p-copying of the pressure the unknown constant c is taken into account. Figures 10 and 11 show the streamlines and isobars in the compound region. The expected recirculation regions are clearly visible, just as is the case with regions of low and high pressure.

The finite volume code is non-stationary and based on pressure correction. The linear systems of equations were solved by a GMRESR iterative solver. The converged results were very similar to the results of the finite element code. In fact the contour plots showed no visible difference. The convergence of the constant c showed exactly the same behaviour as the convergence of

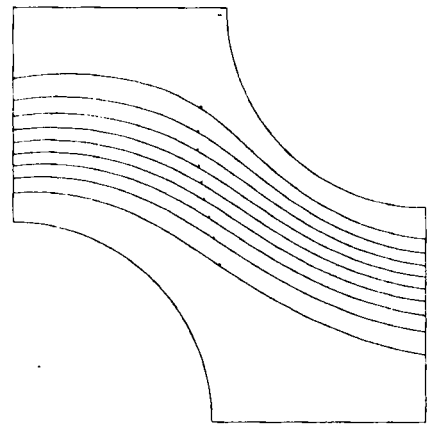

Figure 8. Streamlines in tube problem for $Re_D = 140$

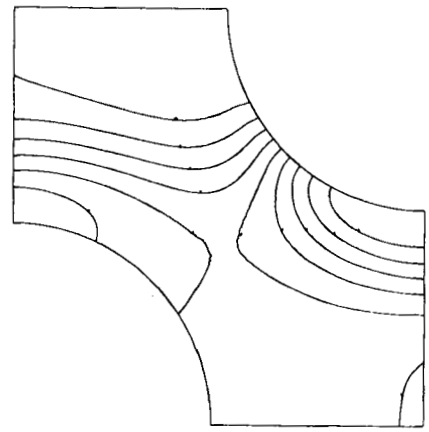

Figure 9. Isobars in tube problem for $Re_D = 140$

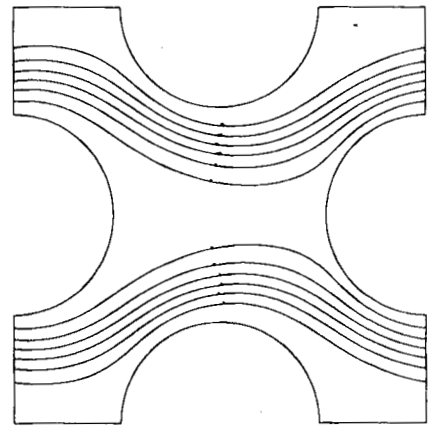

Figure 10. Streamlines in compound region consisting of four computational blocks

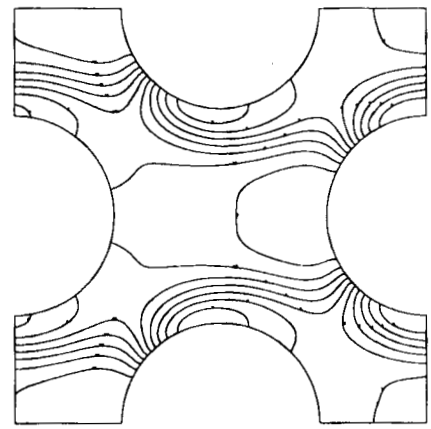

Figure 11. Isobars in compound region consisting of four computational blocks

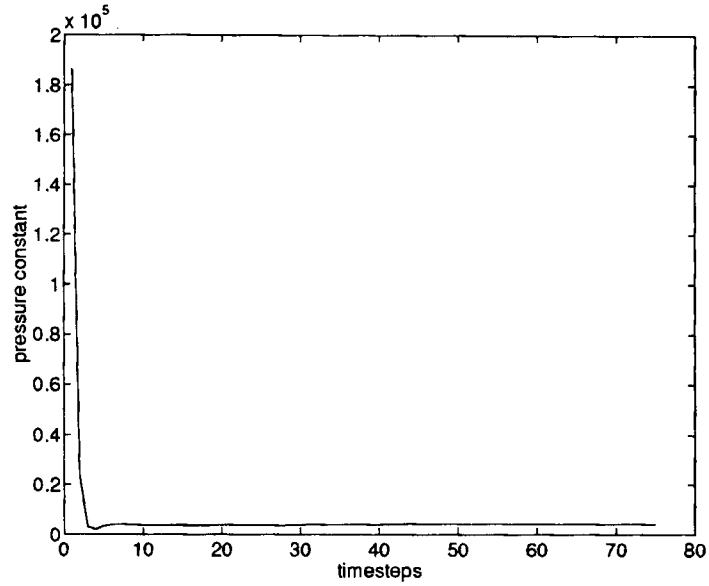

Figure 12. Convergence of unknown constant c as a function of time; $\Delta t = 0{\cdot}001$

the pressure to reach the stationary state. Figure 12 shows the constant c as a function of time. It is clear that our algorithm gives a very good convergence.

To converge to the steady state, 75 time steps $\Delta t = 0{\cdot}001$ s were necessary. The iterative solver for the momentum equations needed approximately 80 iterations for each time step. The number of iterations for the pressure equations was about 100 per time step in the non-preconditioned case. Preconditioning of the pressure matrix as described in Section 4 decreased the average number of iterations to seven. This shows that preconditioning based on the incomplete LU decomposition of the pressure part of (21) and (22) is an excellent preconditioner for the complete system (23b).

6. CONCLUSIONS

Two algorithms to implement periodic and antiperiodic boundary conditions in combination with a given flow rate and an unknown jump in the pressure have been derived. It has been demonstrated that these algorithms converge fast and are very well suited for their purpose. Although both algorithms are completely different and must be applied in different techniques for the solution of the incompressible Navier–Stokes equations, they both converge to exactly the same solution.

REFERENCES

1. C. Cuvelier, A. Segal and A. A. van Steenhoven, *Finite Element Methods and Navier–Stokes Equations*, Reidel, Dordrecht, 1986.
2. A. Fortin, 'On the imposition of a flowrate by an augmented Lagrangian method', *Commun. Appl. Numer. Methods*, **4**, 835–841 (1988).
3. A. E. Mynett, P. Wesseling, A. Segal and C. G. M. Kassels, 'The ISNaS incompressible Navier–Stokes solver: invariant discretization', *Appl. Sci. Res.*, **48**, 175–191 (1991).
4. C. W. Oosterlee and P. Wesseling, 'A multigrid method for an invariant formulation of the incompressible Navier–Stokes equations in general co-ordinates', *Commun. Appl. Numer. Methods*, **8**, 721–734 (1992).

5. M. Perić, 'Finite volume method for the prediction of three-dimensional fluid flow in complex ducts', *Ph.D. Thesis*, Imperial College, London, 1985.
6. A. Segal, P. Wesseling, J. Van Kan, C. W. Oosterlee and K. Kassels, 'Invariant discretization of the incompressible Navier–Stokes equations in boundary fitted co-ordinates', *Int. j. numer. methods fluids*, **15**, 411–426 (1992).
7. D. Simonin and M. Barcouda, 'Measurements and predictions of turbulent flow entering a staggered tube bundle,' *Tech. Rep. H-44/88.25*. EDF, Laboratoire Nationale d'Hydraulique, Chatou, France, 1988.
8. W. Y. Soh and J. W. Goodrich, 'Unsteady solution of incompressible Navier–Stokes equations', *J. Comput. Phys.*, **79**, 113–134 (1988).
9. P. Wesseling, A. Segal, J. J. I. M. Van Kan, C. W. Oosterlee and C. G. M. Kassels, 'Finite volume discretization of the incompressible Navier–Stokes equations in general coordinates on staggered grids', *Comput. Fluid Dyn. J.*, **1**, 27–33 (1992).
10. J. J. I. M. Van Kan, 'A second-order accurate pressure correction method for viscous incompressible flow', *SIAM J. Sci. Stat. Comput.*, **7**, 870–891 (1986).
11. C. Vuik, 'Solution of the discretized incompressible Navier–Stokes equations with the GMRES method', *Int. j. numer. methods fluids*, **16**, 507–523 (1993).